

# MOLECULAR STRUCTURE AND SPECTRA OF DANTHRON AND EMODIN STUDIED BY FTIR, RAMAN SPECTROSCOPY AND DFT TECHNIQUES

B.K. Barik <sup>a</sup>, H.M. Mallya <sup>a</sup>, R.K. Sinha <sup>b</sup>, and S. Chidangil <sup>b</sup>

<sup>a</sup> Department of Biochemistry, Melaka Manipal Medical College (Manipal campus), Manipal Academy of Higher Education, Manipal-576104, Karnataka, India

<sup>b</sup> Department of Atomic and Molecular Physics, Manipal Academy of Higher Education, Manipal-576104, Karnataka, India  
Email: rajeev.sinha@manipal.edu

Received 3 August 2020; revised 16 November 2020; accepted 24 November 2020

In this work, experimental and theoretical studies on danthron and emodin are presented. Experimentally, Fourier transform infrared (FTIR), Raman and UV–Vis spectra of danthron and emodin were recorded. The structure and vibrational frequencies of the molecules were calculated using density functional theory (DFT) with the B3LYP functional using the triple zeta (TZVP) basis set. Among various possible structures of danthron and emodin, it was found that the most stable structures involve intramolecular hydrogen bonds between two OH and C=O groups. The theoretical IR spectra of the most stable conformations of danthron and emodin correlate well with their experimental FTIR. Detailed vibrational frequency analysis was done for all the vibrational modes obtained and were assigned to the ring vibrations along with the stretching and bending of specific bond vibrations. The bands obtained from the experimental FTIR and Raman spectra of both the molecules correlate well with their theoretical data.

**Keywords:** danthron, emodin, Fourier transform infrared (FTIR), density functional theory

## 1. Introduction

Since ancient times anthraquinone derivatives (anthraquinones) obtained from different plant sources have been extensively used as medicines because of their laxative property. Recent studies confirm that these molecules also have anti-inflammatory, analgesic, antimicrobial and antitumor activities [1]. Many traditional Chinese medicines (TCMs) are anthraquinone derivatives in nature. Because of the diversity in their functions these medicines are becoming important sources for potential therapeutic agents. But these medicines generally contain thousands of components. So it becomes very essential to analyse them and find out the exact components that bring out different biological functions. According to their therapeutic potentials different methods have

been used to explore the phytochemical and pharmacological effects of TCMs [2]. Reports suggest that the methanolic extract of rhubarb (traditional Chinese medicine) has phenolic compounds in high concentrations, and also exhibits free radical scavenging actions and shows strong antioxidant properties [3, 4]. The dihydroxy anthraquinones are the major biologically active molecules in rhubarb [4, 5]. One of the dihydroxy anthraquinone derivatives, which is naturally found in barks and roots of many plants and also in Chinese herbs like *Rheum officinale* and *Polygonum cuspidatum*, is emodin that has many therapeutic applications [6]. Many studies have reported about the biological actions of dihydroxy anthraquinones like danthron, physcion, aloe-emodin and chrysophanol. Though there are many investigations done for the functional aspect of these dihydroxy derivatives

of anthraquinones, there are only a few theoretical calculation studies for the structural and spectral properties [7–9]. There are reports that the dihydroxy anthraquinones exhibit a strong intramolecular hydrogen bond [7, 10]. Danthron is one of the simplest anthraquinone derivatives that shows the chromophore framework which is specific to many compounds of pharmaceutical and biological interest.

Theoretical studies such as the geometrical optimization and vibrational spectra calculation of the drugs provide a very good insight for the changes in the conformation [11], reactive nature [12], relationship between the structures and the function [13], and the way in which the drugs interact with other molecules [14]. Previously the ground state geometry optimization used to be done by *ab initio* Hartree–Fock (HF) method. But since many years the density functional theory (DFT) method is the method of choice for the optimization of geometries. In the present study, the dihydroxy anthraquinone derivatives danthron and emodin were optimized by *ab initio* HF and DFT using different basis sets.

To the best of our knowledge, the theoretical IR spectra calculation by DFT using a TZVP basis set, its correlation to experimental IR spectra and the assignments of the calculated vibrational modes of aromatic anthraquinone rings of danthron and emodin have not been reported so far.

The objective of this study is to do the assignments of the vibrational modes obtained from the calculated IR spectra for both the molecules and correlate them with the experimental FTIR spectra. The experimental Raman spectra were also carried out for a comparison purpose. The study further focuses on the calculations of HOMO–LUMO molecular orbitals of danthron and emodin. For knowing the assignments of IR spectra the vibrational frequency calculations are very helpful [15]. Therefore the study gives an insight to the different vibrational assignments of the calculated IR spectra of danthron and emodin.

## 2. Materials and methods

### 2.1. Computational details

The *xyz* coordinates of the dihydroxy anthraquinone derivatives were obtained using the Ar-

gusLab software package [16]. The TmoleX quantum chemical calculation program was used to optimize the ground state geometries using the *xyz* coordinates [17]. Ground state geometric optimizations were performed at HF and DFT (B3LYP) levels. The def-SV(P) basis set was used for HF calculations, whereas the def-SV(P) as well as the triple zeta basis set (TZVP) were used for the DFT calculations for the optimization of ground state geometries. The optimized geometries of danthron and emodin were used to calculate the vibrational spectra by the DFT method. The DFT (B3LYP) method with the TZVP basis set was used for the vibrational (IR) spectra calculation, because IR frequencies are efficiently reproduced by the DFT method [18]. The calculated IR frequencies were corrected using a scaling factor of 0.9778. The assignments of the calculated vibrational frequencies of different vibrational modes along with ring vibrations were carried out based on visual observations using the software TmoleX which is a graphical user interface to the TURBOMOLE quantum chemistry program package [17]. The visual observation provides an insight of the ring vibrations along with different vibrations of bonds. The software TmoleX was also used for visualizing the optimized geometry and the HOMO and LUMO orbitals of the optimized molecules.

### 2.2. Experimental methods

Danthron and emodin were procured from *Sigma-Aldrich* and used as such without any further purification. The infrared spectra of these molecules were recorded using an FTIR spectrometer (*JASCO FT/IR-6300*). A resolution of  $4\text{ cm}^{-1}$  was used by the FTIR spectrometer while recording the spectra. The powder samples of the molecules were mixed separately with KBr to prepare the pellets using the pellet maker (*Technosearch Instruments*). The pellets were kept in the sample holder of the spectrophotometer and the FTIR spectra were recorded.

The Raman spectra were recorded using a home-built micro-Raman spectrometer. For recording the Raman spectra of danthron and emodin, a laser beam of 785 nm wavelength (*Starbright Diode Laser, Torsana Laser Tech, Denmark*) was focused onto the samples by the microscope objective. The laser beam with this particular wavelength was utilized to avoid the laser induced photo-damage

of the sample by shorter wavelengths than this one. Also a longer wavelength helps to reduce the fluorescence effect which can compete with weak Raman signals. But longer wavelengths than this one will reduce the detection efficiency [19, 20]. The spectra were recorded using a 60X microscope objective (*Nikon*, Plan Fluor) with a 0.85 numerical aperture (NA). The spectral resolution of the spectrometer was  $5.7\text{ cm}^{-1}$  (with the spectrometer slit width kept at  $100\text{ }\mu\text{m}$ ) by measuring the FWHM of a  $997\text{ cm}^{-1}$  Raman band of the polystyrene bead spectrum.

The UV–Vis spectrum was recorded using a UV–Visible spectrophotometer (*JASCO*). 1 mg of danthron and emodin samples was mixed with 10 ml methanol separately to produce the stock solution. Then 0.1 ml of these solutions was diluted separately with 2.9 ml of methanol before recording the UV–Vis spectra for both the samples.

### 3. Results and discussion

#### 3.1. Theoretical calculations

##### 3.1.1. Geometry of danthron and emodin

Different ground state optimized conformations obtained for danthron and emodin using HF and DFT (BP86 and B3LYP) methods show that the conformations are similar in different methods and basis sets. It is also noticed that all the converged optimized conformations of danthron and emodin are completely planar in nature. The geometric optimization of danthron (1,8-di-

hydroxy anthraquinone) and emodin (1,3,8-trihydroxy-6-methyl anthraquinone) by the DFT (B3LYP) method with the def-TZVP basis set produced three and eight conformations, respectively (Appendix, Tables A1 and A2). Conformation 1 (Conf-1) of danthron and emodin with two intramolecular hydrogen bonds have the lowest total energy and so the most stable conformers as shown in Fig. 1.

The lowest total energy was always shown by the conformation having the double intramolecular hydrogen bonding by the hydroxyl groups of C1 and C8 with the oxo group of C9. This result correlates with the results of Markovic et al. and Ruifa Jin et al. [7, 10]. The total energies obtained by HF and DFT with different basis sets for danthron explains that the lowest total energy is produced by the conformation 1 with double intramolecular hydrogen bonds. The relative energies by HF and DFT (BP86) with different basis sets clarify that the conformation 1 with one intramolecular hydrogen bond is more stable compared to the conformation 3, which is without any intramolecular hydrogen bond. When the total energies obtained from DFT (BP86) with def-SV(P) and TZVP basis sets were compared, it was clearly evident that the TZVP basis set produces lower total energy as compared to the def-SV(P) basis set for a particular conformation.

When emodin was geometrically optimized at HF and DFT (BP86) levels, eight different conformations were converged. These structures are shown in Appendix, Table A2. The conformations 1, 2, 3 and 4 are closely similar to the conformations 5, 6, 7 and 8, respectively, except the orientation of hydroxyl group on C3.

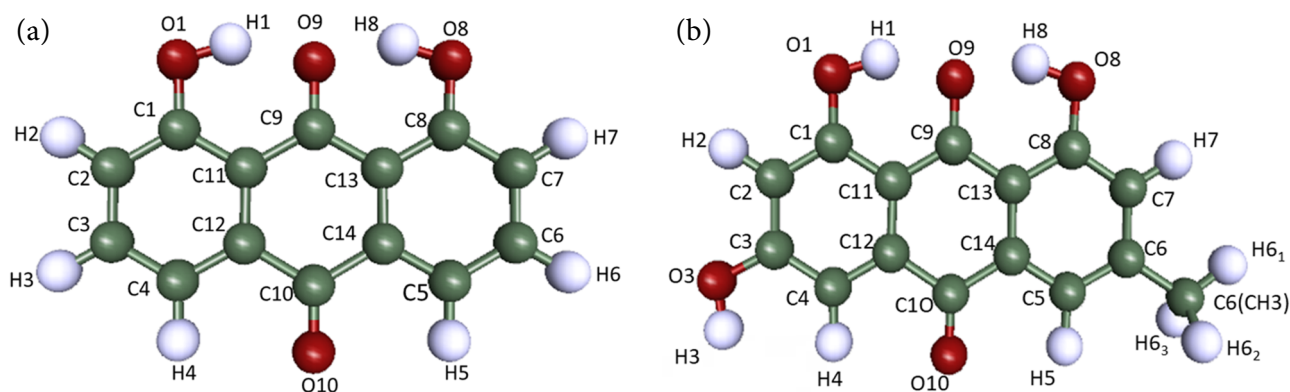


Fig. 1. (a) Conformation 1 of danthron and (b) of emodin having the lowest total energy calculated at DFT (B3LYP) level with def-TZVP basis set.

The total energies show that the lowest total energy is obtained by the conformation 1 using DFT (BP86) with def-SV(P) and TZVP basis sets. The relative energies obtained by using DFT (BP86) with def-SV(P) and TZVP basis sets for the conformation 5 are 0.26 and 0.32 kcal/mol, respectively. But the HF with the def-SV(P) basis set indicates that the conformation 5 has the lowest energy, and the relative energy for the conformation 1 is 0.08 kcal/mol, which is very less when compared with the relative energies produced between the conformations 1 and 5 by DFT. Both the conformations 1 and 5 have double intramolecular hydrogen bonds. The relative energies specify that the conformations 2, 4, 6 and 8 have a similar stability with one intramolecular hydrogen bond and the conformations 3 and 7 are the most unstable conformations without any intramolecular hydrogen bonding.

### 3.1.2. HOMO and LUMO orbitals in danthron and emodin

In all the conformations of danthron the Huckel's method generated 268 molecular orbitals, out of

which 62 were occupied and the rest were unoccupied molecular orbitals. The HOMO and LUMO were calculated by TmoleX using a 3D visualizer. The HOMO and LUMO for the conformation 1 of danthron are shown in Fig. 2(a, b).

When the ground state geometry of emodin was optimized, a total of 300 molecular orbitals were calculated by Huckel's method, out of which only 70 were occupied. The HOMO–LUMO were calculated for emodin by using the 3D visualizer of TmoleX. The HOMO and LUMO for the conformation 1 of emodin are shown in Fig. 3(a, b).

## 3.2. Experimental investigation of danthron

### 3.2.1. UV-Vis spectrum

Theoretical UV-Vis spectrum calculation was done using the DFT method with B3LYP and the def-SVP basis set. For the theoretical calculation the conformation with the lowest total energy was used. The calculated UV-Vis spectrum and the experimental UV-Vis spectrum of danthron are shown in Fig. 4(a, b).

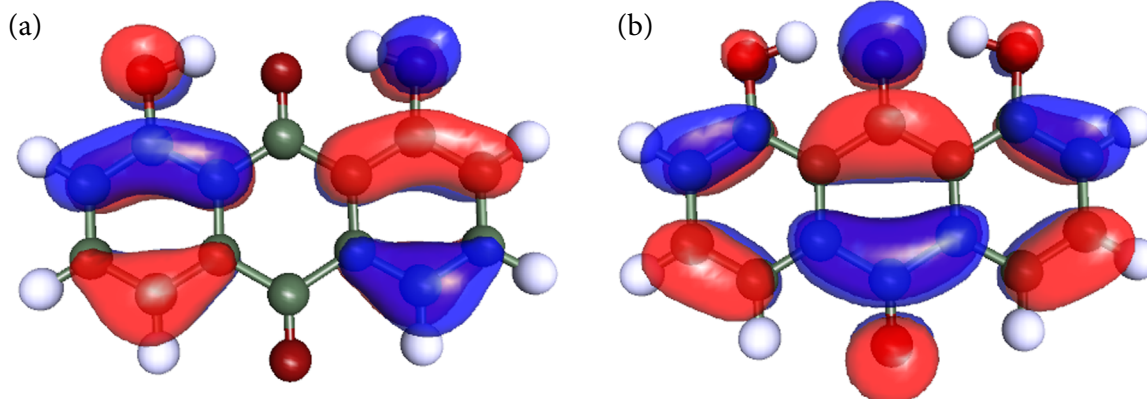


Fig. 2. (a) HOMO and (b) LUMO of danthron calculated with DFT (B3LYP)-def-TZVP.

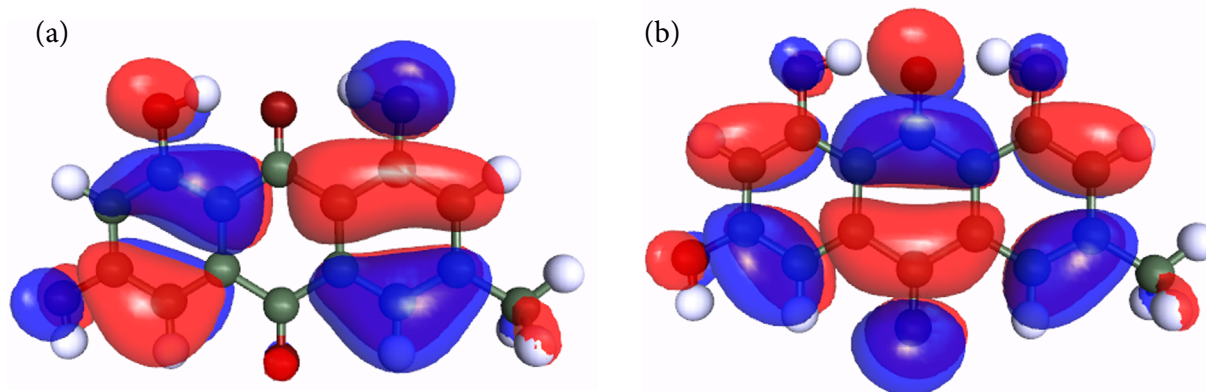


Fig. 3. (a) HOMO and (b) LUMO of emodin calculated with DFT (B3LYP)-def-TZVP.

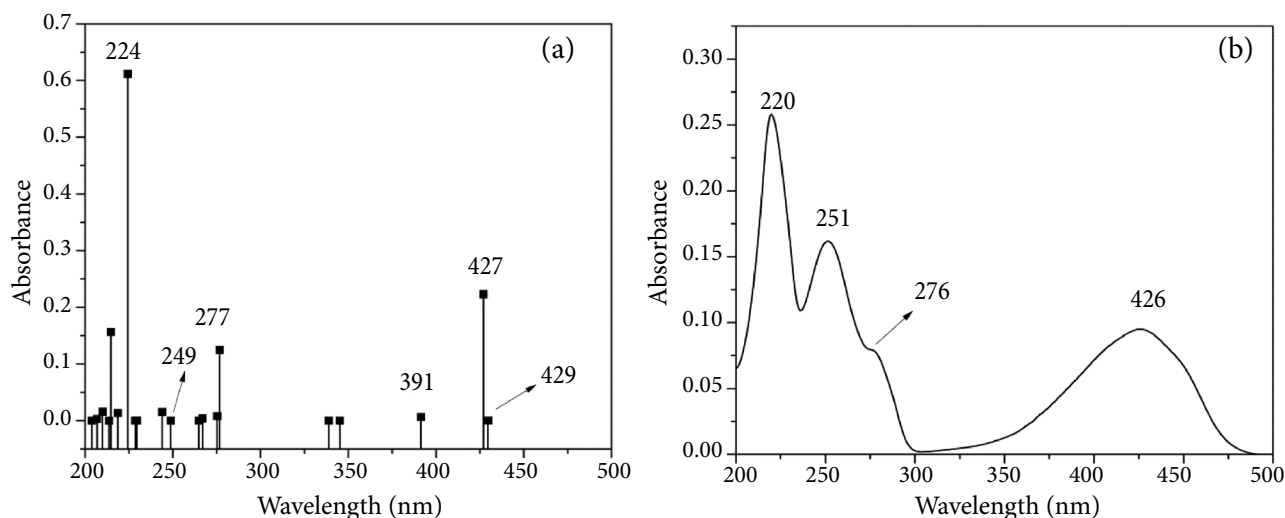


Fig. 4. (a) Calculated UV–Vis spectrum of danthron using DFT (B3LYP) with def-SVP basis set and (b) the experimental UV–Vis spectrum of danthron solution in methanol.

The theoretical and experimental UV–Vis spectra of danthron correlate well with each other.

### 3.2.2. FTIR spectrum of danthron

The FTIR spectrum for danthron is shown in Fig. 5 along with the calculated IR spectrum of the most stable optimized geometry for danthron. From the correlation between the theoretical and the experimental IR spectra, we observed that the calculated IR spectra of the conformer 1 with double intra-molecular hydrogen bonding correlated well with the experimental IR spectrum

whereas the peaks of IR spectrum from the conformer-3 deviate mostly from the peaks of the experimental FTIR spectrum (Appendix, Figs. A1 and A2). Earlier the IR spectrum has been reported by Smulevich et al. [21]. In their work Smulevich et al. have explained two forms of danthron and for the IR frequency assignments they have given the approximate descriptions. In this work after optimizing the geometries for three different conformations their respective IR calculations were done. In our FTIR spectrum a strong and a medium peak were observed at 783 and 456  $\text{cm}^{-1}$ , respectively, which were not present in

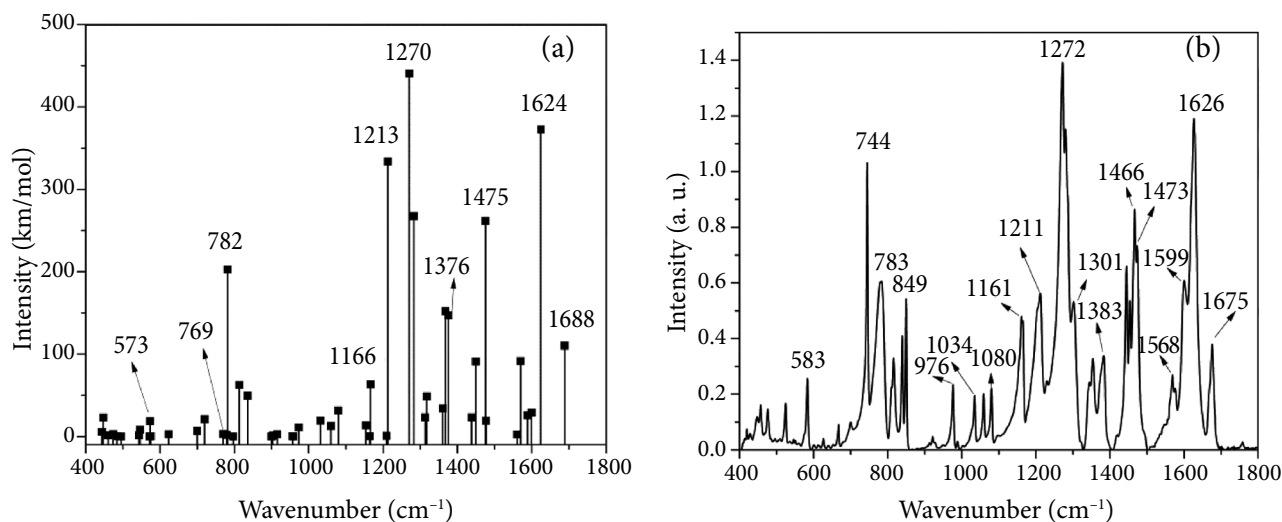


Fig. 5. (a) Theoretically calculated IR spectra of the conformation of danthron having the lowest total energy by DFT method using B3LYP with def-TZVP basis set and (b) the experimental FTIR spectrum of danthron for the correlation.

the previous study. The theoretical calculation correlates these bands with a peak at 782 and 460  $\text{cm}^{-1}$ . The frequency assignment from the theoretical calculation suggested out-of-plane ring deformations for both the bands (Table 1).

### 3.2.3. Raman spectrum of danthron

Previously the Raman spectrum of danthron was reported by Fabriciova et al. [22]. For the comparison purposes we have also recorded the Raman spectrum of danthron which is shown in Fig. 6. As compared to the previous work by Fabriciova et al., we have successfully obtained a greater number of bands than before, i.e. 25 bands vs 16 bands before [22] in the range 1800–400  $\text{cm}^{-1}$ . Among the few new peaks which are present in this Raman spectrum of danthron, the peaks at 1163 and 1341  $\text{cm}^{-1}$  have a strong intensity. Similarly the new bands observed at 741 and 781  $\text{cm}^{-1}$  show a medium intensity. One new weak peak at 1619  $\text{cm}^{-1}$  is observed in this present study which corresponds to the key characteristic very strong FTIR band of danthron at 1626  $\text{cm}^{-1}$ .

### 3.2.4. Vibrational assignments

The theoretical IR calculations of danthron by the DFT (B3LYP) method with the basis set TZVP produced 72 different vibrational modes. Among the 72 vibrational modes, 24 were out-of-plane modes and the rest were in-plane ones.

But in the previous work by Smulevich et al. only three vibrations were assigned as out-of-plane and many assignments were not defined. Here in this work we have mentioned the assignments about all the 72 theoretically obtained IR vibrational frequencies which are shown in Table 1. In Table 1, we have focused to present the theoretical IR vibrational modes with the assignments and their correlation with the corresponding experimental wavenumbers. The previous experimental works on Raman spectra and IR spectra are also mentioned along with the bands obtained in this present work in Table 1.

While visualizing the vibrational modes by the TmoleX program for assignments, we observed different vibrations of the rings of danthron molecule such as stretching, breathing and deformation of rings. In the previous studies, many assignments were mentioned as asymmetric deformity and skeletal deformity. But in our study we have given the complete assignment list with the specification of ring and different individual bond vibrations. Mixtures of both the in-plane and out-of-plane vibrational modes were noticed in a range of 973–45  $\text{cm}^{-1}$ . All the other vibrational modes were in-plane in a range of 3296–1032  $\text{cm}^{-1}$ . Ring deformation was observed in vibrational modes of 208, 314, 335, 443, 447, 1080, 1213, 1270, 1361, 1450 and 1477  $\text{cm}^{-1}$ . In 19 vibrational modes ring breathing was observed, out of which six modes were symmetric ring breathing and thirteen were asymmetric ring breathing.

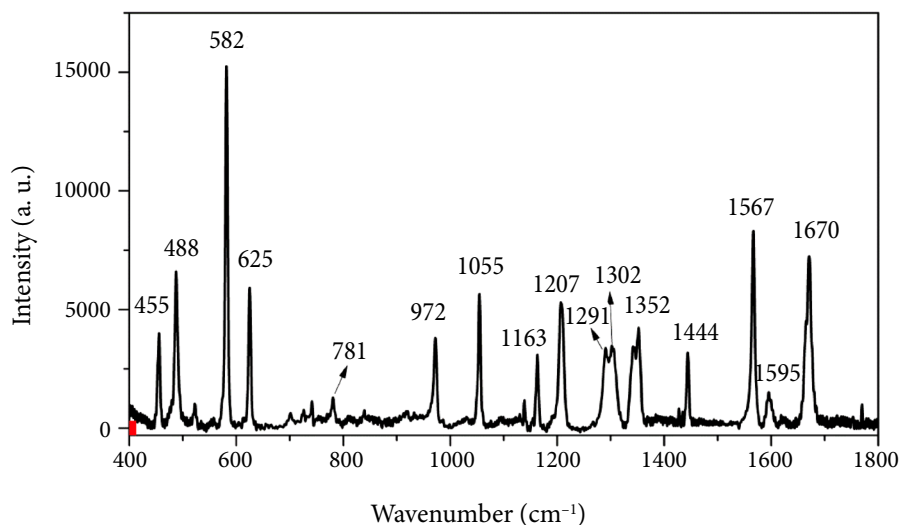


Fig. 6. Raman spectra of danthron (acquisition time 20 s, accumulation 5 and laser power 60 mW).

Table 1. Danthron theoretical IR table with the assignments for the vibrational modes and the correlation of experimental danthron FTIR and Raman data.

Vibrational modes	IR wave-numbers – B3LYP-def-TZVP (cm <sup>-1</sup> ) [this work]	Calculated Raman wavenumbers and calculated assignments in square brackets [22]	Calculated IR frequency assignments [this work]	Experimental IR and its approx. assignment descriptions in square brackets [21]	FTIR [this work]	[This work] Raman frequency and in square brackets Raman by Fabriciova et al. [22]
1	33w		$\gamma$ (Ring deformation)			
2	45w		$\gamma$ (Ring deformation)			
3	71vw		$\gamma$ (Ring deformation)			
4	137w		$\gamma$ (Ring deformation)			
5	174vw		$\gamma$ (Ring deformation)			
6	189vw		$\gamma$ (Ring deformation)			
7	208vw	203vw [ $\delta$ (asymmetric def.)]	Ring deformation			
8	216vw		$\gamma$ (Ring deformation)			
9	280vw	268w [ $\tau$ (asymmetric def.) + $\Omega$ (CCC)]	$\gamma$ (Ring deformation)			
10	314vw		Ring deformation			
11	335w		Ring deformation			
12	364w		Ring stretching			
13	368vw		$\gamma$ (Ring deformation)			
14	443w		Ring stretching		428w	
15	447w		Ring deformation	445m [Skel. Def.]	447m	
16	460w	458vw [ $\delta$ (C–O) + $\delta$ (C=O) + $\delta$ (asymmetric def.)]	$\gamma$ (Ring deformation)		456m	455s [456vw]
		469m [ $\delta$ (asymmetric def.)]				
17	474w	475vw $\tau$ (asymmetric def.)	Ring stretching	473m [ $\delta$ (C=O)]	477m	488vs [487s]
18	484vw		Asy ring breathing			
19	495vw		$\gamma$ (Ring deformation)			
20	543w		Asy ring breathing	522m [Skel. Def. op]	524m	522m
21	546w		$\gamma$ (Ring deformation)	547w [Skel. Def.]	546w	
22	572vw		$\gamma$ (Ring deformation)			
23	573w	574vw [ $\gamma$ (C–O) + $\tau$ (asymmetric def.)]	Sym ring breathing			
24	575vw		$\gamma$ (Ring deformation)	581s [Skel. Def.]	583m	582vs [583m]
25	623w	632vw [ $\gamma$ (COH)]	Asy ring breathing	625w [Skel. Def.]	626w	625vs [626w]
				668m [Skel. Def.]	667m	
26	700w		Ring stretching	699w [218+480–3 <sup>n</sup> ]	700w	701w

Table 1. (continued)

Vibrational modes	IR wave-numbers – B3LYP-def-TZVP (cm <sup>-1</sup> ) [this work]	Calculated Raman wavenumbers and calculated assignments in square brackets [22]	Calculated IR frequency assignments [this work]	Experimental IR and its approx. assignment descriptions in square brackets [21]	FTIR [this work]	[This work] Raman frequency and in square brackets Raman by Fabriciova et al. [22]
27	720w		$\gamma$ (Ring deformation)	708w [ $\gamma$ (CH)]	720w	726w
28	769w		$\gamma$ (Ring deformation)	743vs [ $\gamma$ (CH)]	744vs	741m
29	779w		Asy ring breathing	775s.br [ $\gamma$ (OH), $\gamma$ (OD)]	780s	781m
30	782vs		$\gamma$ (Ring deformation)		783s	
31	797vw		$\gamma$ (Ring deformation)			
32	813m		$\gamma$ (Ring deformation)	812m	816s	
33	836m		Asy ring breathing	839m [Skel. Def.]	839s	839w
				849m [ $\gamma$ (CH)]	849s	
				868w [430×2+8]	867w	
					880w	
34	900vw		$\gamma$ (Ring deformation)		893w	
35	903vw		$\gamma$ (Ring deformation)	910w [430+470+10]	913w	
36	915w		$\gamma$ (Ring deformation)	920w [Skel. Def.]	921w	
37	957vw		$\gamma$ (Ring deformation)			
38	958vw	961m [ $\nu$ (CC)]	$\gamma$ (Ring deformation)			
39	973w		$\gamma$ (Ring deformation)	975m [ $\delta$ (CH)]	976m	972s [976m]
				990w	988w	
40	1032w		Asy ring breathing	1032m [ $\delta$ (CH)]	1034m	
41	1060w	1054w [ $\nu$ (CC)]	Asy ring breathing	1059m [ $\delta$ (CH)]	1059m	1055vs [1059m]
42	1080w		Ring deformation	1079m [Skel. Def.]	1080m	
				1095vw [545×2+5]		1139 m
43	1154w	1144m [ $\delta$ (CH) + $\delta$ (trigonal def.)]	Ring stretching	1155sh [579×2–8]	1153m. sh	1154w [1153m]
44	1164vw		Asy ring breathing	1159/1162m [ $\delta$ (CH)]	1161s	1163 s
45	1166m	1179w [ $\delta$ (CH)]	Ring stretching			
46	1209vw	1203vs [ $\nu$ (CC)]	Asy ring breathing	1205sh [ $\delta$ (OH). $\delta$ (OD)]	1203sh	
47	1213vs		Ring deformation	1210s [Ring st.]	1212	1207vs [1209s]



Table 1. (continued)

Vibrational modes	IR wave-numbers – B3LYP-def-TZVP (cm <sup>-1</sup> ) [this work]	Calculated Raman wavenumbers and calculated assignments in square brackets [22]	Calculated IR frequency assignments [this work]	Experimental IR and its approx. assignment descriptions in square brackets [21]	FTIR [this work]	[This work] Raman frequency and in square brackets Raman by Fabriciova et al. [22]
48	1270vs	1261w [ $\nu$ (CC)]	Ring deformation	1270vs [Ring st.]	1272vs	1291s [1292vs]
49	1283vs		Sym ring breathing	1279vs [ $\nu$ (C–O)]	1279vs	
50	1313w	1308w	Asy ring breathing	1299m [Ring st.]	1301s	1302s [1302vs]
51	1318m	1321vs [ $\nu$ (C–O)]	Asy ring breathing	1345w [Ring st.]	1344m	1341/1345 s
52	1361w	1357m [ $\nu$ (CC) + $\delta$ (C=O) + $\delta$ (asymmetric def.)]	Ring deformation	1358m [ $\nu$ (C–O)]	1353m	1352 vs [1352m]
53	1368s		Sym ring breathing			
54	1376s		Ring stretching	1380sh [Ring st.]	1383m	
				1420vw. sh [1210+214–4]	1418w. sh	
55	1438w		Ring stretching	1442s [Ring st.]	1444s	1444s [1445m]
56	1450m	1453vw [ $\delta$ (CH)]	Ring deformation	1452m [Ring st.]	1454s	
57	1475vs		Sym ring breathing	1465s [Ring st.]	1466s	
58	1477w	1487	Ring deformation	1472m [318+1159–7]	1473s	
59	1561w		Sym ring breathing	1568w [Ring st.]	1568m	1567vs [1569vs]
60	1570m		Ring stretching	1574w [Ring st.]	1576m	
61	1588w	1590vw [ $\nu$ (CC)]	Ring stretching			
62	1599w	1592vw [ $\nu$ (CC)]	Ring stretching	1599m [Ring st.]	1599s	1595m [1601m]
63	1624vs		Sym ring breathing	1625vs [ $\nu$ (C=O)]	1626vs	1619 w
64	1689s	1691vs [ $\nu$ (C=O)]	Asy ring breathing	1672m [ $\nu$ (C=O)]	1675m	1670vs [1675vs]
		1778vs [ $\nu$ (C=O)]				
		3063vs [ $\nu$ (CH)]				

Table 1. (continued)

Vibrational modes	IR wave-numbers – B3LYP-def-TZVP ( $\text{cm}^{-1}$ ) [this work]	Calculated Raman wavenumbers and calculated assignments in square brackets [22]	Calculated IR frequency assignments [this work]	Experimental IR and its approx. assignment descriptions in square brackets [21]	FTIR [this work]	[This work] Raman frequency and in square brackets Raman by Fabriciova et al. [22]
65	3109w		Alternate stretching of [C2–H2 and C7–H7], [C3–H3 and C6–H6] and [C4–H4 and C5–H5]			
66	3110w		Simultaneous stretching of [C2–H2 and C7–H7], [C3–H3 and C6–H6] and [C4–H4 and C5–H5]			
67	3130w		Alternate stretching of [C2–H2 and C7–H7], [C3–H3 and C6–H6] and [C4–H4 and C5–H5]			
68	3131vw		Simultaneous stretching of [C2–H2 and C7–H7], [C3–H3 and C6–H6] and [C4–H4 and C5–H5]			
69	3141w		Alternate stretching of [C2–H2 and C7–H7], [C3–H3 and C6–H6] and [C4–H4 and C5–H5]			
70	3142vw		Simultaneous all C–H stretching			
71	3267vs		Stretching of O1–H1, O8–H8 (Alternatively)			
72	3296w		Stretching of O1–H1, O8–H8 (Simultaneously)			
3553vs [ $\nu$ (OH)]						

$\gamma$ : out of plane vibrational mode, Sym: symmetric and Asy: asymmetric.

The stretching of both the O–H bonds was noticed for only two vibrational modes of 3267 and 3296  $\text{cm}^{-1}$ . The vibrational modes in a range of 3109–3142  $\text{cm}^{-1}$  show mild stretching of few C–H bonds. The vibrational modes that were in a range of 3296–1700  $\text{cm}^{-1}$  produced mainly vibration involving either one single ring or specific bonds without involving any of the rings. The details of all the theoretical vibrational modes of danthron are mentioned in Appendix, Table A3.

### 3.3. Experimental investigation of emodin

#### 3.3.1. UV–Vis spectrum

Theoretical UV–Vis spectrum calculation was done using the DFT method with B3LYP and the def-SVP basis set. For the theoretical calculation the conformation with the lowest total energy was used. The calculated UV–Vis spectrum and the experimental UV–Vis spectrum of emodin are shown in Fig. 7.

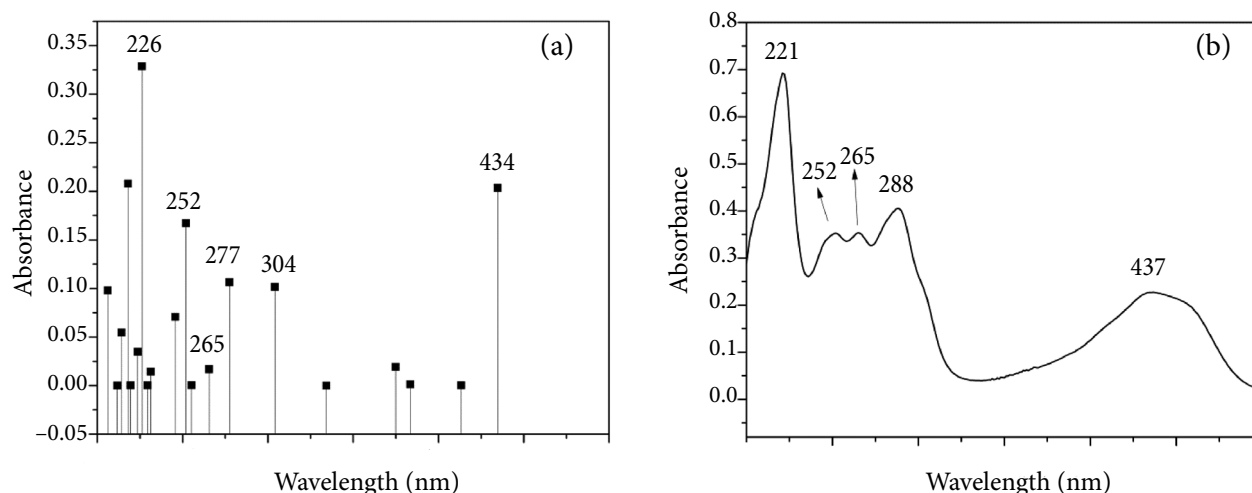


Fig. 7. (a) Calculated UV-Vis spectrum of emodin using the DFT method with B3LYP using def-SVP basis set and (b) the experimental UV-Vis spectrum of emodin solution in methanol.

The theoretical and experimental UV-Vis spectra of danthron correlate well with each other.

### 3.3.2. FTIR spectrum of emodin

From the correlation between the theoretical and the experimental IR spectra, we observed that the calculated IR spectrum of the conformer 1 with double intra-molecular hydrogen bonding correlated well with the experimental IR spectrum. The comparison graph is provided in Appendix, Figs. A3 and A4. The FTIR spectrum for emodin along with the calculated IR spectra of conformer 1 is shown in Fig. 8. The IR spectra of conformations 4 and 6 having one

intra molecular hydrogen bond also correlate with the experimental IR spectrum. But when we compared the IR spectra along with the total energy of the conformations, the conformation 1 with two intra molecular hydrogen bonds has the most stable geometry and correlations to the experimental IR spectrum. Previously the IR and Raman spectra have been reported by Edwards et al. [23]. In their purely experimental work they have shown the IR and Raman spectra of emodin and mentioned the peaks for both the spectra with approximate vibrational assignments. In this present work after optimizing the geometries for eight different conformations of emodin, their respective IR spectra

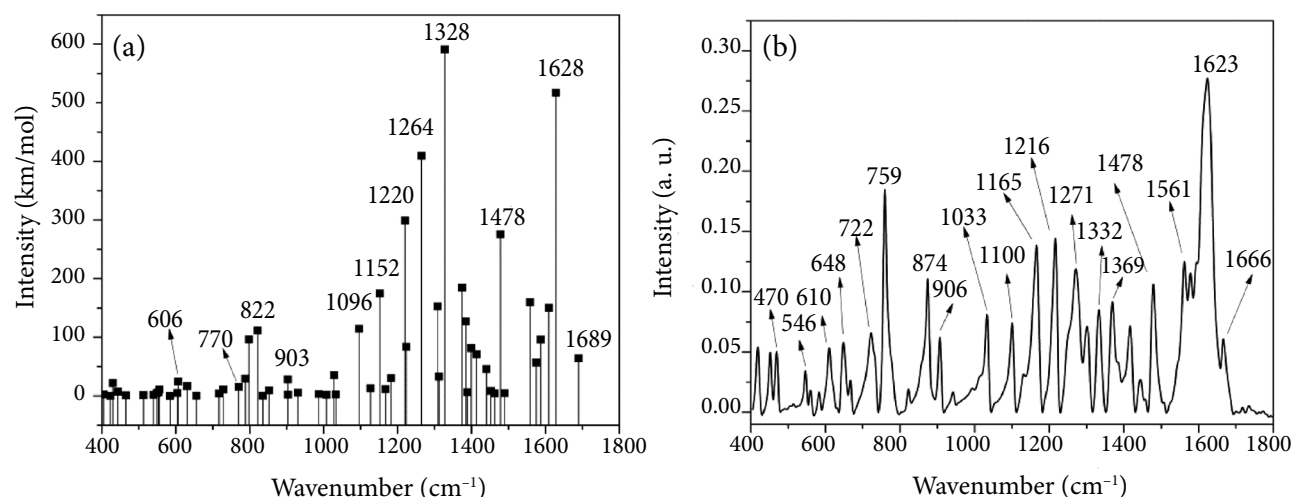


Fig. 8. (a) Theoretically calculated IR spectra of the conformation of emodin having the lowest total energy by DFT method using B3LYP with def-TZVP basis set and (b) the experimental FTIR spectrum of emodin for the correlation.

calculations were done. We were able to observe a total of 38 peaks in the IR spectrum of emodin as compared to 22 peaks observed by the previous work in the 1800–400  $\text{cm}^{-1}$  range. Two peaks out of the 16 new peaks at 1033 and 1594  $\text{cm}^{-1}$  are found to have a strong intensity with out-of-plane ring deformation and a symmetric ring breathing type of vibrations, respectively. Similarly four new peaks at 418, 452, 546 and 648  $\text{cm}^{-1}$  have medium intensity levels with ring deformation ( $\gamma$  mode), asymmetric ring breathing, asymmetric ring stretching and ring deformation ( $\gamma$  mode) types of vibrations, respectively.

### 3.3.3. Raman spectrum of emodin

Previously the Raman spectrum of emodin was reported by Edwards et al. [23]. For the comparison purposes we have also recorded the Raman spectrum of emodin which is shown in Fig. 9. We have successfully obtained a greater number of bands, i.e. 39 bands as compared to 26 bands [23] in the range 1800–400  $\text{cm}^{-1}$ . Out of the 13 new bands one band, i.e. at 456  $\text{cm}^{-1}$ , has a very strong intensity and correlates with the FTIR band of danthron at 452  $\text{cm}^{-1}$  with an asymmetric ring breathing type of vibration. Two other bands at 549 and 1590  $\text{cm}^{-1}$  show medium intensity levels that correlate with the FTIR bands at 549 and 1587  $\text{cm}^{-1}$  having the corresponding assignments of ring deformation ( $\gamma$  mode) and symmetric ring breathing, respectively.

### 3.3.4. Vibrational assignments

The theoretical IR calculation of the emodin molecule by DFT (B3LYP) method with the basis set TZVP produced a total of 84 vibrational modes. The frequency assignments were given for all the 84 vibrational modes, whereas in the previous work done by Edwards et al. [21] only 21 approximate frequency assignments were mentioned for the obtained IR spectrum. Out of the 84 vibrational modes obtained in the present work, the numbers of in-plane and out-of-plane vibrational modes are 43 and 41, respectively. This means that almost 50% of the vibrational modes are out-of-plane that were not found in the case of danthron. In the case of danthron one third of the total vibrational modes were out-of-plane. The increase in the number of out-of-plane vibrational modes may be attributed to the extra two functional groups (OH and  $\text{CH}_3$ ) present in emodin in comparison to danthron.

The theoretical IR values with frequency assignments and the experimental IR values are mentioned in Table 2. Correlation has been done between both the values obtained in the present work along with the previously done work in Table 2. The vibrational modes for each frequency were visualized using the TmoleX for their assignments and that revealed that the ring structure of emodin molecule was exhibiting stretching, deformation, symmetric and asymmetric breathing types of vibrational modes. In a frequency range of

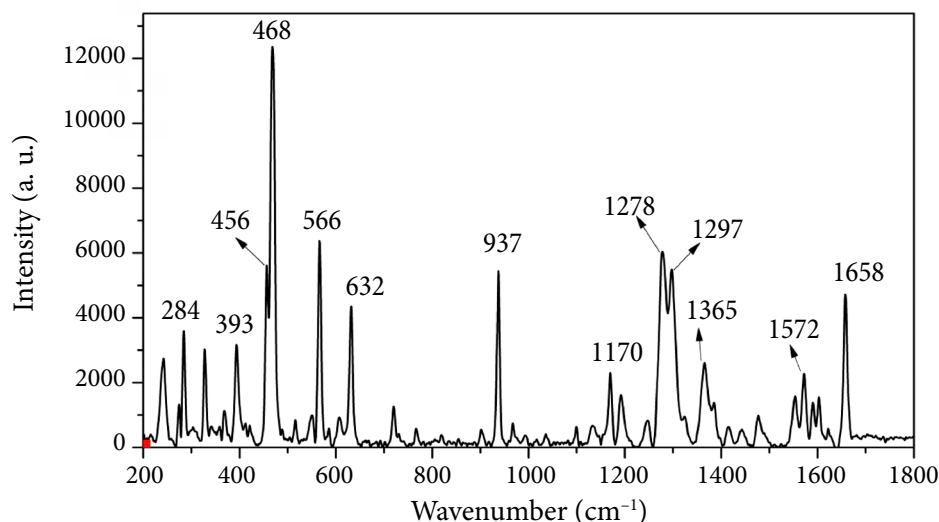


Fig. 9. Raman spectra of emodin (acquisition time 10 s, accumulation 5 and laser power 60 mW).

Table 2. Emodin theoretical IR calculation mentioning their vibrational assignments and the correlation of experimental FTIR and Raman frequencies of emodin.

Vibrational mode	IR wavenumbers – B3LYP-def-TZVP (cm <sup>-1</sup> ) [this work]	Approximate frequency assignment [23]	Calculated IR frequency assignments [this work]	Raman frequency [this work] along with Raman frequency by Edwards et al. [23] in square brackets	FTIR frequency [this work] and IR frequency by Edwards et al. [23] in square brackets
1	30vw		$\gamma^*$ (Ring deformation)		
2	34w		$\gamma$ (Ring deformation)		
3	61vw		$\gamma$ (Ring deformation)		
4	109w		$\gamma$ (Ring deformation)		
5	130vw		$\gamma$ (Ring deformation)		
6	153vw		$\gamma$ (Ring deformation)		
7	167vw		Ring deformation		
8	209w		$\gamma$ (Ring deformation)		
9	213vw		$\gamma$ (Ring deformation)		
10	236vw		$\gamma$ (Ring deformation)		
11	252vw		$\gamma$ (Ring deformation)		
12	253w		$\gamma$ (Ring deformation)		
13	276w		$\gamma$ (Ring deformation)		
14	336w		Ring deformation		
15	364w		Ring stretching		
16	382s		$\gamma$ (One ring with OH group on 3rd carbon deformation)		
17	383w		$\gamma$ (Ring deformation)		
18	405w		$\gamma$ (Ring deformation)		
19	423vw		$\gamma$ (Ring deformation)	421w	418m
20	430w		$\gamma$ (Ring deformation)		
21	443w		$\gamma$ (Ring deformation)	456vs	452m
22	465vw		$\gamma$ (Ring deformation)	468vs [467s]	470m [469w]
23	513w		$\gamma$ (Ring deformation)	516w [519w]	
24	540w		$\gamma$ (Ring deformation)		
25	549w		$\gamma$ (Ring deformation)	549m	546m
26	553w		$\gamma$ (Ring deformation)		
27	555w	Skeletal breathing (565ms)	$\gamma$ (Ring deformation)	566vs [565ms]	560w
28	584vw		$\gamma$ (Ring deformation)	585w	583w
29	604w		$\gamma$ (Ring deformation)		
30	606w	Skeletal deformation (610w)	$\gamma$ (Ring deformation)	607w [612w.sh]	610m [610w]
31	631w	Ring stretch, in-plane (632mw, br)	Sym ring breathing	632vs [632mw.br]	631vw

\* $\gamma$ : out-of-plane vibrational mode, Sym: symmetric and Asy: asymmetric.

Table 2. (continued)

Vibrational mode	IR wavenumbers – B3LYP-def-TZVP (cm <sup>-1</sup> ) [this work]	Approximate frequency assignment [23]	Calculated IR frequency assignments [this work]	Raman frequency [this work] along with Raman frequency by Edwards et al. [23] in square brackets	FTIR frequency [this work] and IR frequency by Edwards et al. [23] in square brackets
32	656vw		$\gamma$ (Ring deformation)	649w	648m
				702w	
33	717w	$\delta$ (C–H) out-of-plane; $\delta$ (OH) phenyl, out-of-plane (720mw, br)	$\gamma$ (Ring deformation)	720m [723vw]	722m [720mw, br]
34	728w		$\gamma$ (Ring deformation)	730w	732w, sh
35	770w	$\nu$ (=C–H) aromatic, out-of-plane (759ms)	Ring deformation	766w	759vs [759ms]
36	788w		$\gamma$ (Ring deformation)		
37	798m		$\gamma$ (Ring deformation)		
38	822s		$\gamma$ (Ring deformation)		822w
39	836vw		$\gamma$ (Ring deformation)		
40	852w		$\gamma$ (Ring deformation)	875w	874s [875mw]
41	903w		$\gamma$ (Ring deformation)		
42	904w		$\gamma$ (Ring deformation)	902w [907vw]	906m [909mw]
43	930w	$\delta$ (C–CH), out-of-plane (942m)	Asy* ring breathing	937vs [942m]	942w
				967w	
44	987w		Asy ring breathing	993w	994w
45	1008w		Asy ring breathing		
46	1028w		Sym* ring breathing		
47	1033w		$\gamma$ (One ring with CH <sub>3</sub> group on C6 carbon deformation)	1035w	1033s
48	1096s	$\delta$ (C–CH), in-plane (1101mw)	Asy ring breathing	1099w [1100vw, br]	1100s [1101mw]
49	1127w	$\delta$ (C–CH), in-plane (1130vw)	Asy ring breathing	1133w [1134vw]	1131m [1130vw]
50	1152s		Ring stretching		
51	1167w	$\delta$ (OH) phenyl, free, in-plane (1167ms)	Asy ring breathing	1170m [1170w]	1165s [1167ms]
52	1182w	Ring stretch, in-plane (1196vw)	Sym ring breathing	1192m [1195vw]	1188vw, sh
53	1220vs	$\nu$ (C–O); $\delta$ (OH) phenyl, in-plane (1217s)	Ring deformation		1216s [1217s]
54	1224m		Asy ring breathing		
		Ring stretch, in-plane (1249vw)		1247w [1249vw]	

\* $\gamma$ : out-of-plane vibrational mode, Sym: symmetric and Asy: asymmetric.

Table 2. (continued)

Vibrational mode	IR wavenumbers – B3LYP-def-TZVP ( $\text{cm}^{-1}$ ) [this work]	Approximate frequency assignment [23]	Calculated IR frequency assignments [this work]	Raman frequency [this work] along with Raman frequency by Edwards et al. [23] in square brackets	FTIR frequency [this work] and IR frequency by Edwards et al. [23] in square brackets
55	1264vs	Ring stretch, in-plane (1271s)	Asy ring breathing	1278vs [1281ms]	1271s [1271s]
56	1308s	Ring stretch, in-plane (1300ms)	Sym ring breathing	1297vs [1298ms]	1301s [1300ms]
57	1312w		Asy ring breathing		
58	1328vs	Ring stretch, in-plane (1333m)	Asy ring breathing	1324w [1325vw]	1332s [1333m]
59	1374s	$\nu$ (C–O) phenyl (1367m)	Asy ring breathing	1365s [1368mw]	1369s [1367m]
60	1384s	$\nu$ (C–O) phenyl (1386m)	Ring stretching	1385m [1380mw]	1383m [1386m]
61	1389w		Asy ring breathing		
62	1399m		Asy ring breathing		
63	1413m	Ring stretch (1413m)	Asy ring breathing	1415w [1417mw]	1416s [1413m]
64	1440m	Ring stretch (1446mw)	Ring stretching	1443w [1446mw]	1443w
65	1452w		$\gamma$ (One ring with CH <sub>3</sub> group on C6 carbon deformation)		1457vw
66	1463w		Asy ring breathing		
67	1478vs	Ring stretch, coupled with	Sym ring breathing	1477w [1479mw]	1478s [1478m]
66	1463w	(OH) (1478m)	Asy ring breathing		
68	1489w		Ring stretching		
69	1558s	$\nu$ (C=C) aromatic (1561mw)	Asy ring breathing	1553m [1557m]	1561s [1561mw]
70	1575m	$\nu$ (C=C) aromatic (1577w)	Sym ring breathing	1572m [1577m]	1578s [1577w]
71	1587m		Sym ring breathing	1590m	1594s
72	1609s	$\nu$ (C=C) aromatic; quadrant ring stretch (1610ms.sh)	Ring stretching	1603m [1607m]	1610vs, sh [1610ms, sh]
73	1628vs	$\nu$ (C=O) conjugated, H-bonded (1628vs)	Sym ring breathing	1622w [1626w.sh]	1623vs [1628vs]
74	1689m	$\nu$ (C=O) conjugated, free (1663w)	Asy ring breathing	1658vs [1659s]	1666m [1663w]
75	2965w	$\nu$ (CH <sub>3</sub> ) asymmetric (2928vw)	Stretching of C6(CH <sub>3</sub> )–H6(1, 2, 3) and C6–C6(CH <sub>3</sub> )		
76	3014w		$\gamma$ [C6(CH <sub>3</sub> )–H6(1, 2) deformation]		

Table 2. (continued)

Vibrational mode	IR wavenumbers – B3LYP-def-TZVP ( $\text{cm}^{-1}$ ) [this work]	Approximate frequency assignment [23]	Calculated IR frequency assignments [this work]	Raman frequency [this work] along with Raman frequency by Edwards et al. [23] in square brackets	FTIR frequency [this work] and IR frequency by Edwards et al. [23] in square brackets
77	3047w	$\nu$ (CH) aromatic (3054vw)	Stretching of C6(CH3)–H6(1, 2, 3)		
78	3112w	$\nu$ (C=CH) aromatic (3080vw)	C4–H4 stretching		
79	3118w		C7–H7 stretching		
80	3124w		C5–H5 stretching		
81	3143vw		C2–H2 stretching		
82	3241vs		Stretching of O1–H1, O8–H8 (Alternatively)		
83	3273m		Stretching of O1–H1, O8–H8 (Simultaneously)		
		$\nu$ (OH) (3389m, br)			
84	3717s		Stretching of O3–H3		

904–30  $\text{cm}^{-1}$ , both in-plane and out-of-plane types of vibrations were observed. But after that in a range of 3717–904  $\text{cm}^{-1}$  mostly in-plane vibrational modes were observed except three vibrational modes at 1033, 1452 and 3014  $\text{cm}^{-1}$ . Ring deformation vibrational modes were both in-plane and out-of-plane. As compared to danthron, the number of asymmetric ring breathing vibrational modes in emodin is greater, i.e. 13 vs 27. The symmetric ring breathings are always in-plane vibrational modes both in danthron and emodin. The two characteristic vibrational frequencies for danthron at 1624 and 1689  $\text{cm}^{-1}$  correlate with the bands in emodin at 1628 and 1689  $\text{cm}^{-1}$  having symmetric and asymmetric ring breathing, respectively. But the FTIR spectra of danthron and emodin show that there is a shift of the band of 1675  $\text{cm}^{-1}$  in danthron to the 1666  $\text{cm}^{-1}$  band of emodin. This shift can be due to the presence of the extra two functional groups in emodin as compared to danthron. The stretching of mainly OH groups is observed at 3241, 3273 and 3717  $\text{cm}^{-1}$ . Like the vibrations of danthron, the vibrational assignments for emodin in the range 3717–1689  $\text{cm}^{-1}$  also produce the vibrations either in one single ring or in some specific bonds only. The details of all the theoretic

cal vibrational modes of emodin are given in Appendix, Table A4.

#### 4. Conclusions

Our theoretical IR calculation studies were performed using the most stable conformations of danthron as well as emodin having the double intramolecular hydrogen bonding. The IR spectra calculated using the DFT (B3LYP) with the def-TZVP basis set relate well with the respective experimental FTIR spectra. Theoretically frequency assignments were allocated for all the vibrational modes. It was observed that there was a clear correlation between the FTIR and Raman spectra with the corresponding theoretical IR spectrum of the most stable conformer. The experimental FTIR and Raman spectra of danthron and emodin show more bands as compared to the previously reported literature data. Some of the newly obtained bands with strong intensity levels are of great importance for the future database. The frequency assignments of danthron and emodin clearly mention the vibrational modes whether in-plane or out-of-plane. Also there is clarity regarding the types of ring vibrations of the molecules. These detailed studies of frequency assignments



on the molecules will be very helpful for the future studies.

### Acknowledgements

The authors are thankful to the FIST program of the Government of India (SR/FST/PSI-174/2012) and the Department of Biotechnology (DBT), Government of India (BT/PR6413/MED/14/802/2005), for the facilities used in the work.

### Appendix

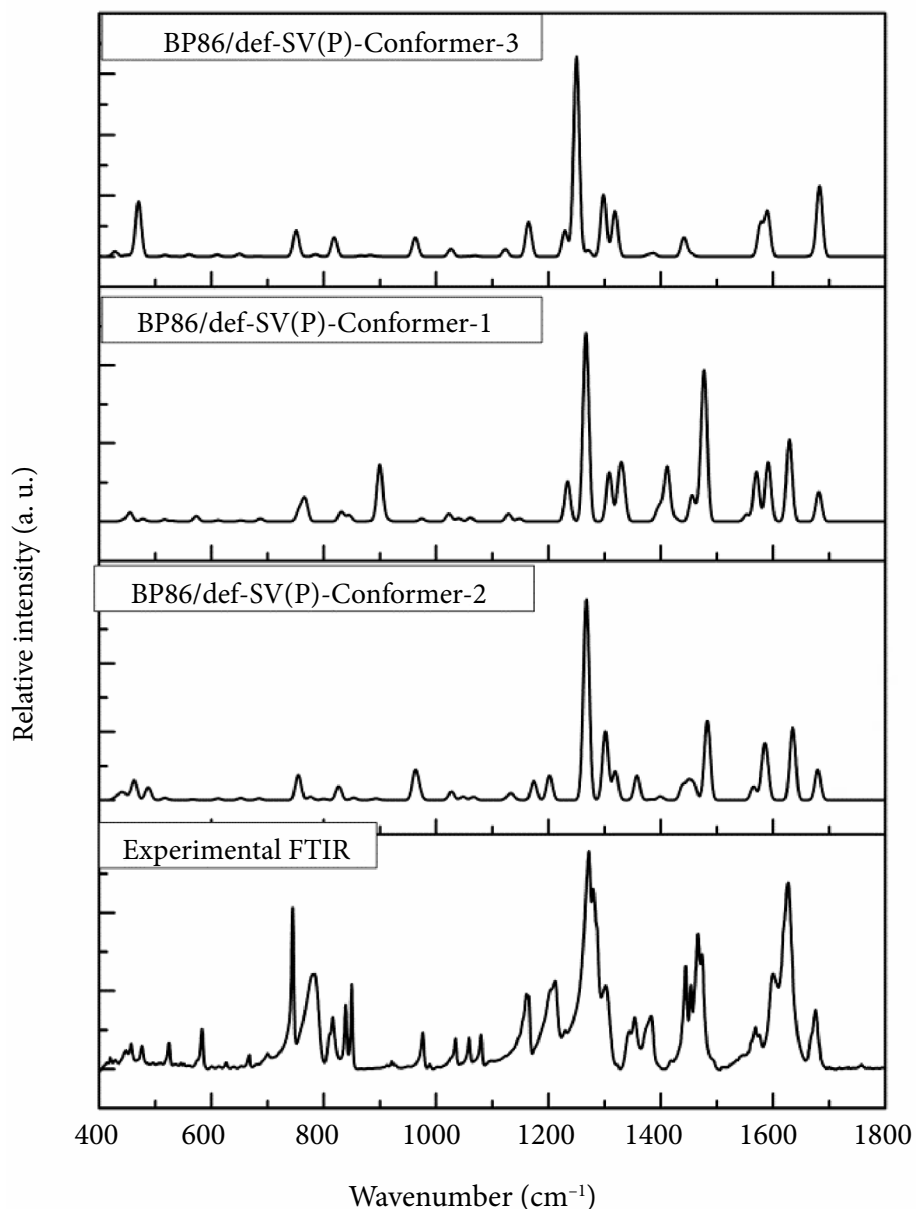


Fig. A1. Theoretical and experimental IR comparison of danthron.

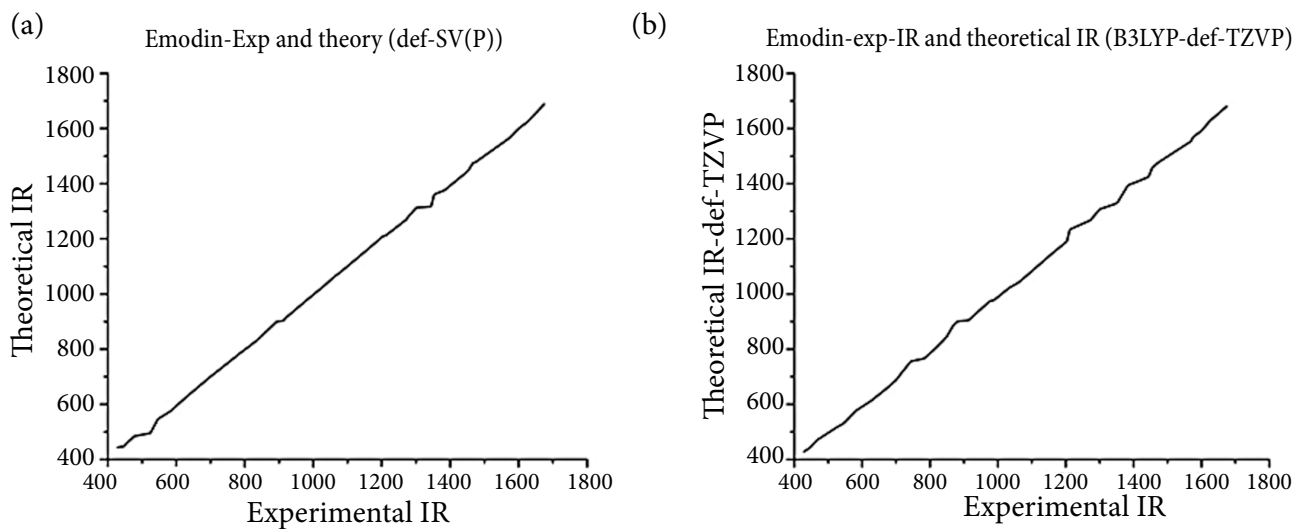


Fig. A2. Correlation graph between the experimental FTIR spectrum and the theoretical IR spectra of danthron by (a) DFT (B3LYP) using TZVP basis set and (b) DFT with BP86 and def-SV(P) basis set.

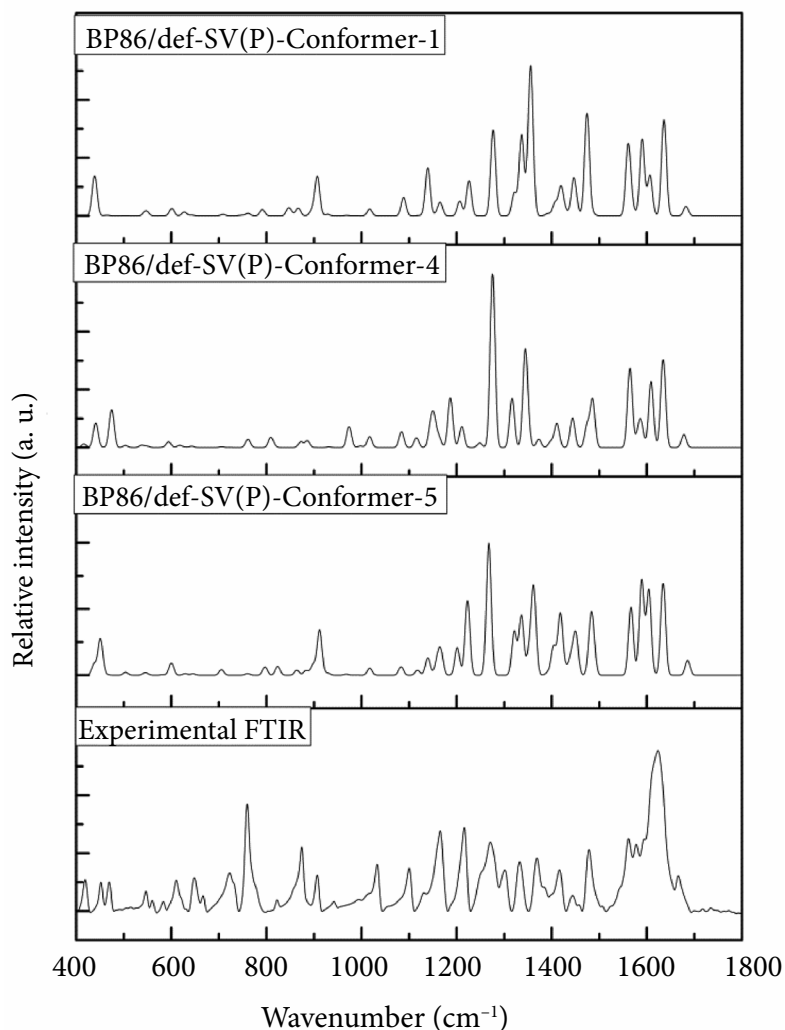


Fig. A3. Comparison of theoretical and experimental emodin IR spectra.

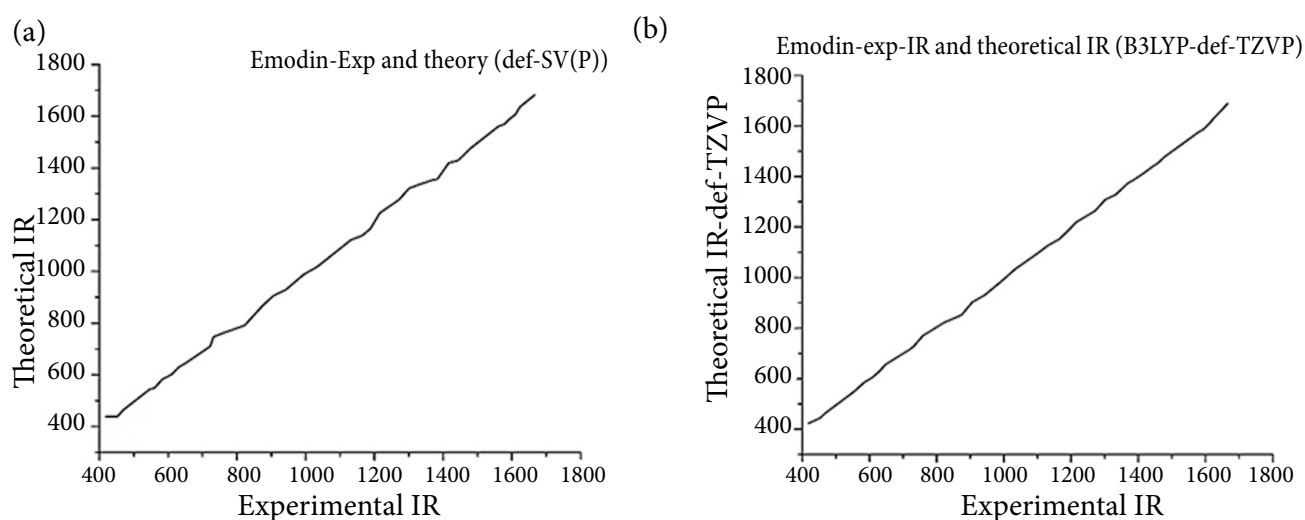


Fig. A4. Correlation graph between the experimental FTIR spectrum and the theoretical IR spectra of emodin by (a) DFT with BP86 and def-SV(P) basis set and (b) DFT with B3LYP and def-TZVP basis sets.

Table A1. Different conformations of danthron with their total energy (TE) and relative energy calculated at HF and DFT (BP86) level with def-SV(P) and TZVP basis set.

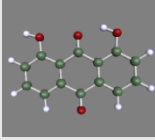
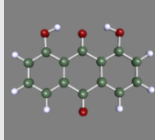
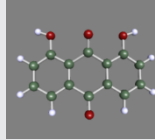
Method				
		1	2	3
HF with def-SV(P) basis set	TE (Hartree)	-833.620029	-833.638059	-833.600770
	Relative energy (kcal/mol)	11.31	0	23.39
DFT (BP86)with def- SV(P) basis set	TE (Hartree)	-838.656440	-838.678801	-838.629784
	Relative energy (kcal/mol)	14.03	0	30.76
DFT (BP86) with TZVP basis set	TE (Hartree)	-839.566836	-839.587766	-839.541888
	Relative energy (kcal/mol)	13.13	0	28.79

Table A2. Different conformations of emodin with total energy (TE) and relative energy calculated at HF and DFT (BP86) level with def-SV(P) and TZVP basis sets.

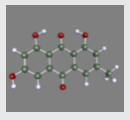
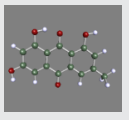
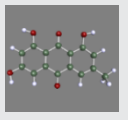
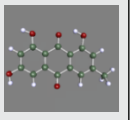
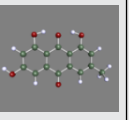
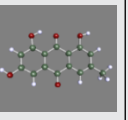
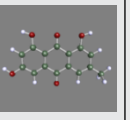
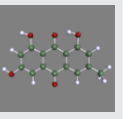
Method									
	1	2	3	4	5	6	7	8	
HF with def-SV(P) basis set	TE (Hartree)	-947.439852	-947.420929	-947.400895	-947.421061	-947.439977	-947.421061	-947.398713	-947.419650
	Relative energy (kcal/mol)	0.08	11.95	24.52	11.87	0	11.87	25.89	12.75
DFT (BP86) with def-SV(P) basis set	TE (Hartree)	-953.137295	-953.114130	-953.087037	-953.113843	-953.136877	-953.113843	-953.084647	-953.112100
	Relative energy (kcal/mol)	0	14.54	31.54	14.72	0.26	14.72	33.04	15.81
DFT (BP86) with TZVP basis set	TE (Hartree)	-954.184127	-954.162526	-954.136982	-954.162130	-954.183612	-954.162130	-954.134635	-954.160383
	Relative energy (kcal/mol)	0	13.55	29.58	13.80	0.32	13.80	31.05	14.90

Table A3. Details of danthron IR assignments.

Vibrational modes	IR wavenumbers – B3LYP-def-TZVP (cm <sup>-1</sup> ) [this work]	Calculated IR frequency assignments [this work]
1	33w	$\gamma$ (Ring deformation)
2	45w	$\gamma$ (Ring deformation) + $\gamma$ (deformation of C=O, C–H and O–H)
3	71vw	$\gamma$ (Ring deformation)
4	137w	$\gamma$ (Ring deformation) + $\gamma$ (C10=O10 deformation)
5	174vw	$\gamma$ (Ring deformation) + $\gamma$ (C=O deformation)
6	189vw	$\gamma$ (Ring deformation)
7	208vw	Ring deformation
8	216vw	$\gamma$ (Ring deformation) + $\gamma$ (C4–H4, C5–H5 and C–O deformation)
9	280vw	$\gamma$ (Ring deformation) + $\gamma$ (C9=O9 deformation) + $\gamma$ (C4–H4 and C5–H5 deformation) + $\gamma$ (C1–O1 and C8–O8 deformation)
10	314vw	Ring deformation + C10=O10 deformation
11	335w	Ring deformation
12	364w	Ring stretching + C10=O10 deformation
13	368vw	$\gamma$ (Ring deformation) + $\gamma$ (C3–H3, C6–H6 and C–O deformation)
14	443w	Ring stretching + [O–H and C–O stretching]

Table A3. (continued)

Vibrational modes	IR wavenumbers – B3LYP-def-TZVP (cm <sup>-1</sup> ) [this work]	Calculated IR frequency assignments [this work]
15	447w	Ring deformation + C=O deformation + $\beta$ (O–H) + $\beta$ (C–O)
16	460w	$\gamma$ (Ring deformation) + $\gamma$ (C9=O9 deformation) + $\gamma$ (C3–H3, C6–H6 and C–O deformation)
17	474w	Ring stretching + C9=O9 deformation + $\beta$ (O–H)
18	484vw	Asy ring breathing + C9=O9 stretching + C–O stretching
19	495vw	$\gamma$ (Ring deformation) + $\gamma$ (C–H deformation)
20	543w	Asy ring breathing + C=O stretching + stretching of C–O + stretching of C2–H2, C3–H3, C6–H6 and C7–H7
21	546w	$\gamma$ (Ring deformation) + $\gamma$ (C=O deformation) + $\gamma$ (C2–H2, C3–H3, C6–H6, C7–H7 deformation) + $\gamma$ (O–H deformation) + $\gamma$ (C–O deformation)
22	572vw	$\gamma$ (Ring deformation) + $\gamma$ (C9=O9 deformation) + $\gamma$ (C–H deformation) + $\gamma$ (C–O deformation)
23	573w	Sym ring breathing + stretching of C2–H2 and C7–H7 + stretching of O–H and C–O + $\beta$ (C–O)
24	575vw	$\gamma$ (Ring deformation) + $\gamma$ (C=O deformation) + $\gamma$ (C2–H2, C7–H7 deformation) + $\gamma$ (O–H deformation)
25	623w	Asy ring breathing + $\beta$ (C3–H3 and C6–H6) + stretching of C9=O9 and C–O
26	700w	Ring stretching + C=O deformation + $\beta$ (C4–H4 and C5–H5) + stretching of O–H
27	720w	$\gamma$ (Ring deformation) + $\gamma$ (C=O deformation) + $\gamma$ (C3–H3, C4–H4, C5–H5, C6–H6 deformation) + $\gamma$ (O–H deformation) + $\gamma$ (C–O deformation)
28	769w	$\gamma$ (Ring deformation) + $\gamma$ (C–H deformation) + $\gamma$ (O–H deformation) + $\gamma$ (C–O deformation)
29	779w	Asy ring breathing + C9=O9 stretching + $\beta$ (C4–H4 and C5–H5) + C–H and C–O stretching
30	782vs	$\gamma$ (Ring deformation) + $\gamma$ (C10=O10 deformation) + $\gamma$ (C–H deformation) + $\gamma$ (O–H deformation)
31	797vw	$\gamma$ (Ring deformation) + $\gamma$ (C–H deformation) + $\gamma$ (O–H deformation)
32	813m	$\gamma$ (Ring deformation) + $\gamma$ (C–H deformation) + $\gamma$ (C=O deformation) + $\gamma$ (O–H deformation)
33	836m	Asy ring breathing + C=O deformation + $\beta$ (C3–H3, C4–H4, C5–H5, C6–H6)
34	900vw	$\gamma$ (Ring deformation) + $\gamma$ (C–H deformation) + $\gamma$ (O–H and C–O deformation)
35	903vw	$\gamma$ (Ring deformation) + $\gamma$ (C–H deformation) + $\gamma$ (C10=O10 deformation) + $\gamma$ (O–H deformation)
36	915w	$\gamma$ (Ring deformation) + $\gamma$ (C–H deformation) + $\gamma$ (C=O deformation) + $\gamma$ (O–H deformation)
37	957vw	$\gamma$ (Ring deformation) + $\gamma$ (C–H deformation)
38	958vw	$\gamma$ (Ring deformation) + $\gamma$ (C–H deformation)
39	973w	$\gamma$ (Ring deformation) + $\gamma$ [deformation of C=O and C–H]
40	1032w	Asy ring breathing + C=O deformation + $\beta$ (C–H)
41	1060w	Asy ring breathing + stretching of C=O + $\beta$ (C–H) + $\beta$ (O–H)
42	1080w	Ring deformation + C=O deformation + $\beta$ (C–H) + $\beta$ (O–H)
43	1154w	Ring stretching + $\beta$ (C–H) + $\beta$ (O–H) + stretching of C9=O9
44	1164vw	Asy ring breathing + $\beta$ (C–H) + $\beta$ (O–H) + stretching of C=O
45	1166m	Ring stretching + $\beta$ (C–H) + $\beta$ (O–H) + C=O deformation
46	1209vw	Asy ring breathing + $\beta$ (C–H) + $\beta$ (O–H) + stretching of C9=O9
47	1213vs	Ring deformation + $\beta$ (C–H) + $\beta$ (O–H) + C9=O9 deformation

Table A3. (continued)

Vibrational modes	IR wavenumbers – B3LYP-def-TZVP ( $\text{cm}^{-1}$ ) [this work]	Calculated IR frequency assignments [this work]
48	1270vs	Ring deformation + $\beta$ (C–H) + $\beta$ (O–H) + C10=O10 stretching + C9=O9 deformation
49	1283vs	Sym ring breathing + $\beta$ (C–H) + $\beta$ (O–H) + stretching of C9=O9
50	1313w	Asy ring breathing + stretching of C9=O9 + $\beta$ (C–H) + $\beta$ (O–H)
51	1318m	Asy ring breathing + stretching of C9=O9 + $\beta$ (C–H) + $\beta$ (O–H) + deformation of C10=O10
52	1361w	Ring deformation + deformation of C=O + $\beta$ (O–H) + $\beta$ (C2–H2, C3–H3, C6–H6, C7–H7)
53	1368s	Sym ring breathing + $\beta$ (O–H) + stretching of C2–H2 and C7–H7 + stretching of C=O + $\beta$ (C3–H3, C4–H4, C5–H5, C6–H6)
54	1376s	Ring stretching + $\beta$ (C3–H3, C4–H4, C5–H5, C6–H6) + C9=O9 deformation + $\beta$ (O–H)
55	1438w	Ring stretching + $\beta$ (C–H) + $\beta$ (O–H) + stretching of C9=O9
56	1450m	Ring deformation + $\beta$ (C2–H2, C3–H3, C6–H6, C7–H7) + $\beta$ (O–H)
57	1475vs	Sym ring breathing + $\beta$ (C–H) + $\beta$ (O–H) + stretching of C=O
58	1477w	Ring deformation + $\beta$ (C3–H4, C4–H4, C5–H5, C6–H6) + $\beta$ (O–H)
59	1561w	Sym ring breathing + $\beta$ (C–H) + $\beta$ (O–H) + stretching of C=O
60	1570m	Ring stretching + $\beta$ (O–H) + stretching of C3–H3 and C6–H6 + $\beta$ (C2–H2, C4–H4, C5–H5, C7–H7)
61	1588w	Ring stretching + $\beta$ (O–H) + stretching of C3–H3, C4–H4, C5–H5 and C6–H6, stretching of C=O
62	1599w	Ring stretching + $\beta$ (O–H) + $\beta$ (C2–H2, C4–H4, C5–H5, C7–H7)
63	1624vs	Sym breathing of ring + $\beta$ (O–H) + $\beta$ (C2–H2, C7–H7) + stretching of C=O
64	1689s	Asy ring breathing + stretching of C2–H2, C7–H7, C4–H4 and C5–H5 + $\beta$ (O–H) + stretching of C10=O10 + $\beta$ (C3–H3, C6–H6)

$\beta$ : in-plane bending.

Table A4. Details of emodin IR assignments.

Vibrational mode	Wavenumbers [this work] ( $\text{cm}^{-1}$ )	Calculated IR frequency assignments [this work]
1	30vw	$\gamma$ (Ring deformation) + $\gamma$ [C6(CH3)–H6(1, 2, 3)] deformation
2	34w	$\gamma$ (Ring deformation) + $\gamma$ (C10=O10 deformation) + $\gamma$ [C6(CH3)–H6(1, 2, 3)] deformation
3	61vw	$\gamma$ (Ring deformation), $\gamma$ [deformation of C6–C6 (CH3)]
4	109w	$\gamma$ (Ring deformation) + $\gamma$ (deformation of C=O) + $\gamma$ (deformation of C–H)
5	130vw	$\gamma$ (Ring deformation) + $\gamma$ (deformation of C=O) + $\gamma$ (deformation of C2–H2 and C7–H7) + $\gamma$ [deformation of C6–C6(CH3)] + $\gamma$ [C6(CH3)–H6(1, 2, 3) deformation]
6	153vw	$\gamma$ (Ring deformation) + $\gamma$ [C6–C6(CH3) deformation] + $\gamma$ [C6(CH3)–H6(1, 2, 3) deformation] + $\gamma$ [C2–H2 and C7–H7 deformation]
7	167vw	Ring deformation + stretching of [C6–C6(CH3) + O–H + C6(CH3)–H6(1, 2, 3) + C4–H4 and C5–H5]
8	209w	$\gamma$ (Ring deformation) + $\gamma$ (O3–H3 deformation) + $\gamma$ (C–H deformation)
9	213vw	$\gamma$ (Ring deformation) + $\gamma$ (C4–H4 and C6–H6 deformation) + $\gamma$ (O3–H3 deformation)
10	236vw	$\gamma$ (Ring deformation) + $\gamma$ [deformation of C6–C6(CH3) + C=O + C6(CH3)–H6(1, 2, 3) + O1–H1 + C4–H4, C5–H5 and C7–H7]

Table A4. (continued)

Vibrational mode	Wavenumbers [this work] (cm <sup>-1</sup> )	Calculated IR frequency assignments [this work]
11	252vw	$\gamma$ (Ring deformation) + $\gamma$ [deformation of C=O + C3-O3+ C6-C6(CH3) + C6(CH3)-H6(1, 2)]
12	253w	$\gamma$ (Ring deformation) + $\gamma$ [deformation of C-O + C6-C6(CH3) + C=O + O3-H3 + C2-H2, C4-H4 and C7-H7]
13	276w	$\gamma$ (Ring deformation) + $\gamma$ [deformation of C-O + C10=O10 + O-H]
14	336w	Ring deformation) + [stretching of C1-O1 + C8-O8 + C6-C6(CH3) + C6(CH3)-H6(1)]
15	364w	Ring stretching + $\beta$ (C10=O10) + $\beta$ (C8-O8) + stretching of (O8-H8), C6-C6(CH3) and C6(CH3)-H6(1, 2, 3)
16	382s	$\gamma$ (Asy one ring deformation) + $\gamma$ ( deformation of O3-H3)
17	383w	$\gamma$ (Asy one ring deformation) + $\gamma$ [deformation of O3-H3 + C10=O10 + C1-O1 + O1-H1 + C3-O3 and O3-H3]
18	405w	$\gamma$ (Ring deformation) + $\gamma$ [deformation of C10=O10 + C2-H2 and C7-H7]
19	423vw	$\gamma$ (Ring deformation) + $\gamma$ [deformation of C9=O9 + C2-H2 and C7-H7]
20	430w	$\gamma$ (Ring deformation) + $\gamma$ [deformation of C=O + O1-H1 + O8-H8 + C3-O3]
21	443w	$\gamma$ (Ring deformation) + $\gamma$ [deformation of O-H + C4-H4 + C5-H5 and C6-C6(CH3)]
22	465vw	$\gamma$ (Ring deformation) + $\gamma$ [deformation of C2-H2 + C7-H7 + O1-H1 + O8-H8 + C6-C6(CH3)]
23	513w	$\gamma$ (Ring deformation) + $\gamma$ [deformation of C-O + O-H + C9=O9 + C6-C6(CH3) + C2-H2 and C7-H7 + C6(CH3)-H6(1, 2, 3)]
24	540w	$\gamma$ (Ring deformation) + $\gamma$ [deformation of C-O + C9=O9 + C2-H2 and C5-H5 + C6-C6(CH3) and C6(CH3)-H6(1, 2, 3)]
25	549w	$\gamma$ (Ring deformation) + $\gamma$ [deformation of C-O + C2-H2 and C2-H5 + C6-C6(CH3) and C6(CH3)-H6(1, 2, 3)]
26	553w	$\gamma$ (Ring deformation) + $\gamma$ [deformation of C2-H2 + C6(CH3)-H6(1, 2, 3) and C=O]
27	555w	$\gamma$ (Ring deformation) + $\gamma$ [deformation of C9=O9 + O-H + C-O and C6-C6(CH3)]
28	584vw	$\gamma$ (Ring deformation) + $\gamma$ [deformation of C7-H7 + C8-O8 and C9=O9]
29	604w	$\gamma$ (Ring deformation) + $\gamma$ [deformation of C3-O3 + C9=O9 + C4-H4, O-H and C6-C6(CH3)]
30	606w	$\gamma$ (Ring deformation) + $\gamma$ [deformation of C3-O3 + C6-C6(CH3) + C9=O9 + O1-H1 + O8-H8 + C4-H4 and C5-H5]
31	631w	Sym ring breathing + stretching of O-H, C2-H2 + C7-H7 and C6-C6(CH3)
32	656vw	$\gamma$ (Ring deformation) + $\gamma$ [deformation of C=O + C4-H4 and O-H]
33	717w	$\gamma$ (Ring deformation) + $\gamma$ [deformation of C9=O9 + C3-O3 + C6-C6(CH3) + C4-H4 and C5-H5]
34	728w	$\gamma$ (Ring deformation) + $\gamma$ [deformation of C=O + C4-H4 + C5-H5 + C2-H2 and C7-H7]
35	770w	Ring deformation + [stretching of C=O + C5-H5 + C-O + C6-C6(CH3) + O3-H3] + $\gamma$ (stretching of C4-H4)
36	788w	$\gamma$ (Ring deformation) + $\gamma$ [deformation of O1-H1 + O8-H8 + C2-H2, C4-H4, C5-H5 and C7-H7]
37	798m	$\gamma$ (Ring deformation) + $\gamma$ [deformation of O1-H1, O8-H8, C2-H2, C4-H4, C5-H5 and C7-H7]
38	822s	$\gamma$ (Ring deformation) + $\gamma$ [deformation of C2-H2 + C5-H5 + C7-H7 + C4-H4 + O1-H1 + O8-H8 and C9=O9]
39	836vw	$\gamma$ (Ring deformation) + $\gamma$ [deformation of C2-H2 + C5-H5 + C7-H7 + C4-H4 + O1-H1 + O8-H8 and C6(CH3)-H6(1, 2, 3)]
40	852w	$\gamma$ (Ring deformation) + $\gamma$ [deformation of C10=O10+ O1-H1+ O3-H3 + C2-H2 + C4-H4 and C7-H7]

Table A4. (continued)

Vibrational mode	Wavenumbers [this work] (cm <sup>-1</sup> )	Calculated IR frequency assignments [this work]
41	903w	$\gamma$ (Ring deformation) + $\gamma$ [deformation of C9=O9 + C1-O1 + C8-O8 + O-H + C2-H2 + C7-H7 + C5-H5 + C6(CH3)-H6(1, 2, 3) and C6-C6(CH3)]
42	904w	$\gamma$ (Ring deformation) + $\gamma$ [deformation of C4-H4 + C5-H5 + C7-H7 and O8-H8]
43	930w	Asy ring breathing + stretching of C6-C6(CH3), C-O and O1-H1
44	987w	Asy ring breathing + stretching of C6(CH3)-H6(1, 2, 3), C6-C6(CH3), C-O, C5-H5 and $\beta$ [C6(CH3)-H6(1, 2, 3)]
45	1008w	Asy ring breathing + stretching of C2-H2, C4-H4, C7-H7, C6-C6(CH3), C6(CH3)-H6(1, 2, 3) and C-O
46	1028w	Sym ring breathing + $\beta$ (C-H) + $\beta$ (O3-H3) + C10=O10 deformation + stretching of C6-C6(CH3)
47	1033w	$\gamma$ (One ring deformation) + $\gamma$ [deformation of C5-H5 + C7-H7 + C6-C6(CH3) and C6(CH3)-H6(1, 2, 3)]
48	1096s	Asy ring breathing + $\beta$ (C4-H4, C5-H5 and C7-H7) + $\beta$ (O3-H3) + $\beta$ [C6(CH3)-H6(1, 2, 3)], C=O deformation, stretching of C1-O1, C8-O8 and C6-C6(CH3)
49	1127w	Asy ring breathing + $\beta$ (C5-H5, C7-H7 and C4-H4) + $\beta$ (O8-H8 and O3-H3) + $\beta$ [C6(CH3)-H6(1)] + stretching of C6-C6(CH3) and C9=O9
50	1152s	Asy ring stretching + $\beta$ (O3-H3) + $\beta$ (C2-H2 and C7-H7), stretching of C3-O3, C1-O1 and C6-C6(CH3)
51	1167w	Asy ring breathing + $\beta$ (O-H) + $\beta$ (C2-H2, C4-H4, C5-H5 and C7-H7), C10=O10 deformation and stretching of C-O, C9=O9 and C6-C6(CH3)
52	1182w	Sym ring breathing + $\beta$ (C4-H4, C5-H5 and C7-H7) + C10=O10 deformation + $\beta$ (O3-H3) + stretching of C-O and C9=O9
53	1220vs	Ring deformation + $\beta$ (C2-H2, C5-H5 and C7-H7) + $\beta$ (O-H) + C=O deformation + $\beta$ [C6(CH3)-H6(1, 2, 3)], $\beta$ [C1-O1, C8-O8 and C6-C6(CH3)] + stretching of C3-O3
54	1224m	Asy ring breathing + $\beta$ (O-H) + $\beta$ (C2-H2, C4-H4, C5-H5 and C7-H7), stretching of C-O, C6-C6(CH3) and C9=O9
55	1264vs	Asy ring breathing + $\beta$ (C2-H2, C4-H4, C5-H5 and C7-H7), $\beta$ (O-H), C=O deformation, $\beta$ [C6(CH3)-H6(1, 2)] + stretching of C-O and C6-C6(CH3)
56	1308s	Sym ring breathing + $\beta$ (O1-H1 and O8-H8) + $\beta$ (C4-H4), $\beta$ [C6-C6(CH3)], $\beta$ [C6(CH3)-H6(1, 2, 3)] + stretching of C9=O9 and C-O + deformation of C10=O10
57	1312w	Asy ring breathing + $\beta$ (O-H) + $\beta$ (C-H) + $\beta$ [C6(CH3)-H6(1, 2, 3)] + $\beta$ [C6-C6(CH3)] and stretching of C-O and C9=O9
58	1328vs	Asy ring breathing + $\beta$ (O-H) + deformation of C=O + $\beta$ [C6(CH3)-H6(1, 2, 3)] + $\beta$ (C4-H4 and C5-H5) and stretching of C-O
59	1374s	Asy ring breathing + $\beta$ (O3-H3 and O8-H3) + $\beta$ [C6-C6(CH3)], $\beta$ (C2-H2 and C7-H7), C=O deformation, $\beta$ [C6(CH3)-H6(1, 2)]
60	1384s	Ring stretching + $\beta$ (O-H) + deformation of C9=O9 + $\beta$ (C2-H2) + $\beta$ [(CH3)6-H6(1, 2)], $\beta$ [C6-C6(CH3)] and stretching of C-O and C10=O10
61	1389w	Asy one ring breathing + $\beta$ [C6(CH3)-H6(1, 2, 3)] + $\beta$ (C4-H4 and C7-H7), stretching of C6-C6(CH3), C8-O8 and C9=O9
62	1399m	Asy ring breathing + $\beta$ (C-H) + $\beta$ (O1-H1 and O3-H3) + $\beta$ [C6(CH3)-H6(1, 2, 3)] + $\beta$ [C6-C6(CH3)] deformation of C9=O9 and stretching of C10=O10
63	1413m	Asy ring breathing + $\beta$ [(CH3)6-H6(1, 2, 3)] + $\beta$ [O-H] + $\beta$ (C4-H4, C7-H7 and C5-H5) + deformation of C9=O9 + $\beta$ [C6-C6(CH3)]



Table A4. (continued)

Vibrational mode	Wavenumbers [this work] (cm <sup>-1</sup> )	Calculated IR frequency assignments [this work]
64	1440m	Asy ring stretching + $\beta$ (O1–H1 and O3–H3), $\beta$ (C–H), C9=O9 deformation + $\beta$ (C3–O3) + $\beta$ [(CH3)6–H6(1, 2, 3)] + stretching of C1–O1, C8–O8 and C6–C6(CH3) and deformation of C10=O10
65	1452w	$\gamma$ (Mild one ring deformation) + $\gamma$ [deformation of (CH3)6–H6(1, 2, 3)]
66	1463w	Asy ring breathing + $\beta$ (O–H) + $\beta$ (C–H) + $\beta$ [C6(CH3)–H6(1, 2, 3)], stretching of C9=O9, C–O and C6–C6(CH3)
67	1478vs	Sym ring breathing + $\beta$ (O–H) + $\beta$ (C–H) + $\beta$ [C6(CH3)–H6(1, 2, 3)] stretching of C–O, C=O and C6–C6(CH3)
68	1489w	Ring stretching + $\beta$ (C4–H4 and C5–H5) + $\beta$ (O1–H1 and O8–H8), stretching of C–O, C6–C6(CH3) and C9=O9
69	1558s	Asy ring breathing + $\beta$ (O8–H8) + $\beta$ (C4–H4 and C7–H7) + $\beta$ (O3–H3), stretching of C=O, C6(CH3)–H6(1, 2, 3) and C6–C6(CH3)
70	1575m	Sym ring breathing + $\beta$ (O–H) + $\beta$ (C–H) and stretching of C=O and C6–C6(CH3)
71	1587m	Sym ring breathing + $\beta$ (O–H) + $\beta$ (C4–H4 and C5–H5) + $\beta$ [C6–C6(CH3)], $\beta$ [C6(CH3)–H6(1, 2, 3)] and stretching of C=O
72	1609s	Ring stretching + $\beta$ (C–H) + $\beta$ (O–H) + $\beta$ [C6(CH3)–H6(1, 2, 3)], C=O deformation and stretching of C6–C6(CH3)
73	1628vs	Sym ring breathing + $\beta$ (C–H) + $\beta$ (OH) + $\beta$ [C6(CH3)–H6(1, 2, 3)] + stretching of C6–C(CH3) and C=O
74	1689m	Asy ring breathing + stretching of C10=O10, C6–C(CH3) + $\beta$ (O–H) + $\beta$ (C–H) + C6(CH3)–H6(1, 2, 3)

## References

- [1] D.S. Alves, L. Pérez–Fons, A. Estepa, and V. Micol, Membrane–related effects underlying the biological activity of the anthraquinones emodin and barbaloin, *Biochem. Pharmacol.* **68**(3), 549–561 (2004).
- [2] X. Huang, L. Kong, X. Li, X. Chen, M. Guo, and H. Zou, Strategy for analysis and screening of bioactive compounds in traditional Chinese medicines, *J. Chromatogr. B* **812**(1–2), 71–84 (2004).
- [3] H. Matsuda, T. Morikawa, I. Toguchida, J.–Y. Park, S. Harima, and M. Yoshikawa, Antioxidant constituents from rhubarb: structural requirements of stilbenes for the activity and structures of two new anthraquinone glucosides, *Bioorg. Med. Chem.* **9**(1), 41–50 (2001).
- [4] Y. Cai, Q. Luo, M. Sun, and H. Corke, Antioxidant activity and phenolic compounds of 112 traditional Chinese medicinal plants associated with anticancer, *Life Sci.* **74**(17), 2157–2184 (2004).
- [5] C.H. Xiao, S.S. Yang, and X.K. Hong, *The Chemistry of Traditional Chinese Medicines* (Shanghai Science and Technology Publishing Press, Shanghai, 2000).
- [6] B.A. Monisha, N. Kumar, and A.B. Tikku, in: *Anti–inflammatory Nutraceuticals and Chronic Diseases* (Springer, Cham, 2016) pp. 47–73.
- [7] R. Jin and H. Bao, A DFT study on the radical scavenging activity of hydroxyanthraquinone derivatives in rhubarb, *Int. J. Quantum Chem.* **111**(5), 1064–1071 (2011).
- [8] S.Z. Marković and N.T. Manojlović, DFT study on the reactivity of OH groups in emodin: structural and electronic features of emodin radicals, *Monatsh. Chem.* **140**(11), 1311 (2009).
- [9] Z. Marković, N. Manojlović, and S. Zlatanović, Electronic absorption spectra of substituted anthraquinones and their simulation using ZINDO/S method, *J. Serbian Soc. Comput. Mech.* **2**(2), 73–79 (2008).
- [10] Q. Zhang, X. Gong, H. Xiao, and X. Xu, Density functional theory study on anthraquinone and its hydroxyl derivatives, *Acta Chim. Sinica* **64**(5), 381 (2006).

- [11] I.M. Kenawi, DFT analysis of diclofenac activity and cation type influence on the theoretical parameters of some diclofenac complexes, *J. Mol. Struct. Theochem* **761**(1–3), 151–157 (2006).
- [12] H.N. Flores and M.D. Glossman, CHIH–DFT determination of the electrical, optical, and magnetic properties and NICS aromaticity of megazol, *J. Mol. Struct. Theochem* **717**(1–3), 1–3 (2005).
- [13] P.G. De Benedetti, G. Pier, S. Quartieri, and A. Rastelli, A theoretical study of the structure–activity relationship in sulpha drugs, *J. Mol. Struct. Theochem* **85**(1–2), 45–51 (1981).
- [14] Y.B. Shankar Rao, M.V.S. Prasad, N. Udaya Sri, and V. Veeraiah, Vibrational (FT–IR, FT–Raman) and UV–Visible spectroscopic studies, HOMO–LUMO, NBO, NLO and MEP analysis of benzyl (imino (1H–pyrazol–1–yl) methyl) carbamate using DFT calculations, *J. Mol. Struct.* **1108**, 567–582 (2016).
- [15] A.M. Mansour, Coordination behavior of sulfamethazine drug towards Ru (III) and Pt (II) ions: Synthesis, spectral, DFT, magnetic, electrochemical and biological activity studies, *Inorg. Chim. Acta* **394**, 436–445 (2013).
- [16] M.A. Thompson, in: *Proceedings of ACS Meeting*, Vol. 172 (Philadelphia, 2004) p. 42.
- [17] *TURBOMOLE V6.2010*, a development of University of Karlsruhe and Forschungszentrum Karlsruhe GmbH, 1989–2007 (TURBOMOLE GmbH, since 2007), <https://www.turbomole.com>
- [18] M. Büschel, Ch. Stadler, Ch. Lambert, M. Beck, and J. Daub, Heterocyclic quinones as core units for redox switches: UV–vis/NIR, FTIR spectroelectrochemistry and DFT calculations on the vibrational and electronic structure of the radical anions, *J. Electroanal. Chem.* **484**(1), 24–32 (2000).
- [19] A. Bankapur, E. Zachariah, S. Chidangil, M. Valiathan, and D. Mathur, Raman tweezers spectroscopy of live, single red and white blood cells, *PLoS One* **5**(4), e10427 (2010).
- [20] R.D. Snook, T.J. Harvey, E.C. Faria, and P. Gardner, Raman tweezers and their application to the study of singly trapped eukaryotic cells, *Integr. Biol.* **1**(1), 43–52 (2009).
- [21] G. Smulevich and M.P. Marzocchi, Single crystal and polarized infrared spectra of two forms of 1,8–dihydroxyanthraquinone vibrational assignment and crystal structures, *Chem. Phys.* **94**(1–2), 99–108 (1985).
- [22] G. Fabriciova, J.V. García-Ramos, P. Miskovsky, and S. Sanchez-Cortes, Adsorption and acidic behavior of anthraquinone drugs quinizarin and danthron on Ag nanoparticles studied by Raman spectroscopy, *Vib. Spectrosc.* **34**(2), 273–281 (2004).
- [23] H.G.M. Edwards, E.M. Newton, D.D. Wynn–Williams, and S.R. Coombes, Molecular spectroscopic studies of lichen substances 1: parietin and emodin, *J. Mol. Struct.* **648**(1–2), 49–59 (2003).

## DANTRONO IR EMODINO MOLEKULINĖS SANDAROS IR SPEKTRŲ TYRIMAI FTIR, RAMANO SPEKTROKOPIJOS IR TANKIO FUNKCIONALO METODAIS

B.K. Barik<sup>a</sup>, H.M. Mallya<sup>a</sup>, R.K. Sinha<sup>b</sup>, S. Chidangil<sup>b</sup>

<sup>a</sup> *Manipalo aukštojo mokslo akademijos Melakos Manipalo medicinos kolegijos Biochemijos skyrius, Manipalas, Karnataka, Indija*

<sup>b</sup> *Manipalo aukštojo mokslo akademijos Atoaminės ir molekulinės fizikos skyrius, Manipalas, Karnataka, Indija*